

Figure S1. Deletion of AGK in macrophages leads to enhanced anti-tumor activity

(A, B) qRT-PCR and immunoblotting analysis of the expression of AGK in *Agk^{fl/fl}* or *Agk^{CKO}* macrophages (n = 3 per group). (C) H&E and TUNEL, Ki67 staining of tumor tissues from LLC-bearing *Agk^{fl/fl}* and *Agk^{CKO}* mice. (D) CD31 (Red) / α -SMA (Green) double immunostaining of tumor tissues from LLC-bearing *Agk^{fl/fl}* and *Agk^{CKO}* mice. (E-F) The percentages of M1 (CD11C⁺CD206⁻) or M2 (CD11C⁻CD206⁺) among gated F4/80⁺CD11b⁺ macrophages in tumor tissues from LLC-bearing *Agk^{fl/fl}* and *Agk^{CKO}* mice were determined and quantified by flow cytometry (n = 5). Data were shown as mean \pm SEM and were analyzed by unpaired two-tailed t-test (A, D, F). Data in (A-F) are representative of three independent experiments; ns, no significance; **p* < 0.05, ***p* < 0.01, ****p* < 0.001.

Figure S2. Deficiency of AGK in macrophages enhances T cell anti-tumor response

(A) Flow gating strategy for cytokines and cell surface staining in CD8⁺ T cells in *Agk^{fl/fl}* or *Agk^{CKO}* B16-OVA melanoma-bearing mice. (B, C) Representative percentages and immunofluorescence staining of CD4⁺ T cell and CD8⁺ T cell in LLC tumor tissues from *Agk^{fl/fl}* and *Agk^{CKO}* tumor mice (n \geq 5 per group). (D) Representative plots and percentages of PD1⁺Tim3⁺CD8⁺ T cells in the tumor tissues from *Agk^{fl/fl}* and *Agk^{CKO}* LLC-bearing mice (n \geq 4 per group). (E) Representative plots and percentages of CD4⁺ Foxp3⁺ T cells population. (F) Representative plots of CD4⁺ T cells and CD8⁺ T cells isolated from LLC tissues of *Agk^{fl/fl}* and *Agk^{CKO}* mice treated with PBS or anti-CD4/8 antibody (n \geq 3 per group). Data were means \pm SEM and were analyzed by two-tailed, unpaired Student's *t*-test (B-E). Data were representative of one (E, F) or three (B, D) experiments. ns, no significance; **p* < 0.05; ***p* < 0.01, ****p* < 0.001.

Figure S3. AGK deficiency in macrophage enhances CD8⁺ T cell stemness

(A, B) Representative plots and percentages of PD1⁺Tcf1⁺Tim3⁻CD8⁺ T cells population determined by flow cytometry in LLC-bearing *Agk^{fl/fl}* and *Agk^{CKO}* mice (n = 6 per group). Data were shown as means \pm SEM and were analyzed by two-tailed, unpaired Student's *t*-test (B). Data were representative of two (A, B) experiments. ns, no significance; **p* < 0.05; ***p* < 0.01, ****p* < 0.001.

Figure S4. Macrophage AGK deficiency promotes cGAS-STING signaling pathway and type I IFN response

(A-F) The expressions of Type I IFN related genes were determined by RT-PCR in *Agk^{fl/fl}* and *Agk^{CKO}* BMDMs upon treatment with B16-TCM (B16 CM:DMEM = 0: 1; 1: 5; 1: 3) for 6 h. (G) Immunoblot analysis of the amounts of (AGK, cGAS, p-Tbk1, Tbk1, p-IRF3, IRF3, p-P65, P65 and STING) in *Agk^{fl/fl}* and *Agk^{CKO}* BMDMs that were treated with B16F10-TCM (LLC CM:DMEM = 1: 3) for 0, 30, 60, 120 and 180 min. Data were means \pm SEM and were analyzed by and two-way ANOVA (A-F). Data were representative of two (G) or three (A-F) experiments. ns, no significance; **p* < 0.05; ***p* < 0.01; ****p* < 0.001.

Figure S5. AGK-deficient macrophages promote the anti-tumor effects by inducing mitochondrial ROS and enhancing cGAS-STING-type I IFN response

(A) 5×10^5 LLC cells were subcutaneously injected into *Agk^{fl/fl}* and *Agk^{CKO}* mice that were treated with PBS or anti-IFNAR antibody i.p 250 μ g at day 2, 4, 7 and 11 and the tumor volumes were measured at the indicated times (n = 5 per group). Flow cytometric analysis and the percentages of CD107a⁺CD8⁺ T cells in four groups were quantified.

(B) *Agk^{fl/fl}* or *Agk^{KO}* BMDMs were cultured with or without Mito-TEMPO (500 μ M) for 24 h and MitoSOX levels were determined by flow cytometry. Data were means \pm SEM and were analyzed by two-tailed, unpaired Student's *t*-test (A) or two-way ANOVA (B). Data were representative of one (A) or three (B) experiments. ns, no significance; * $p < 0.05$; ** $p < 0.01$; *** $p < 0.001$.

Figure S1

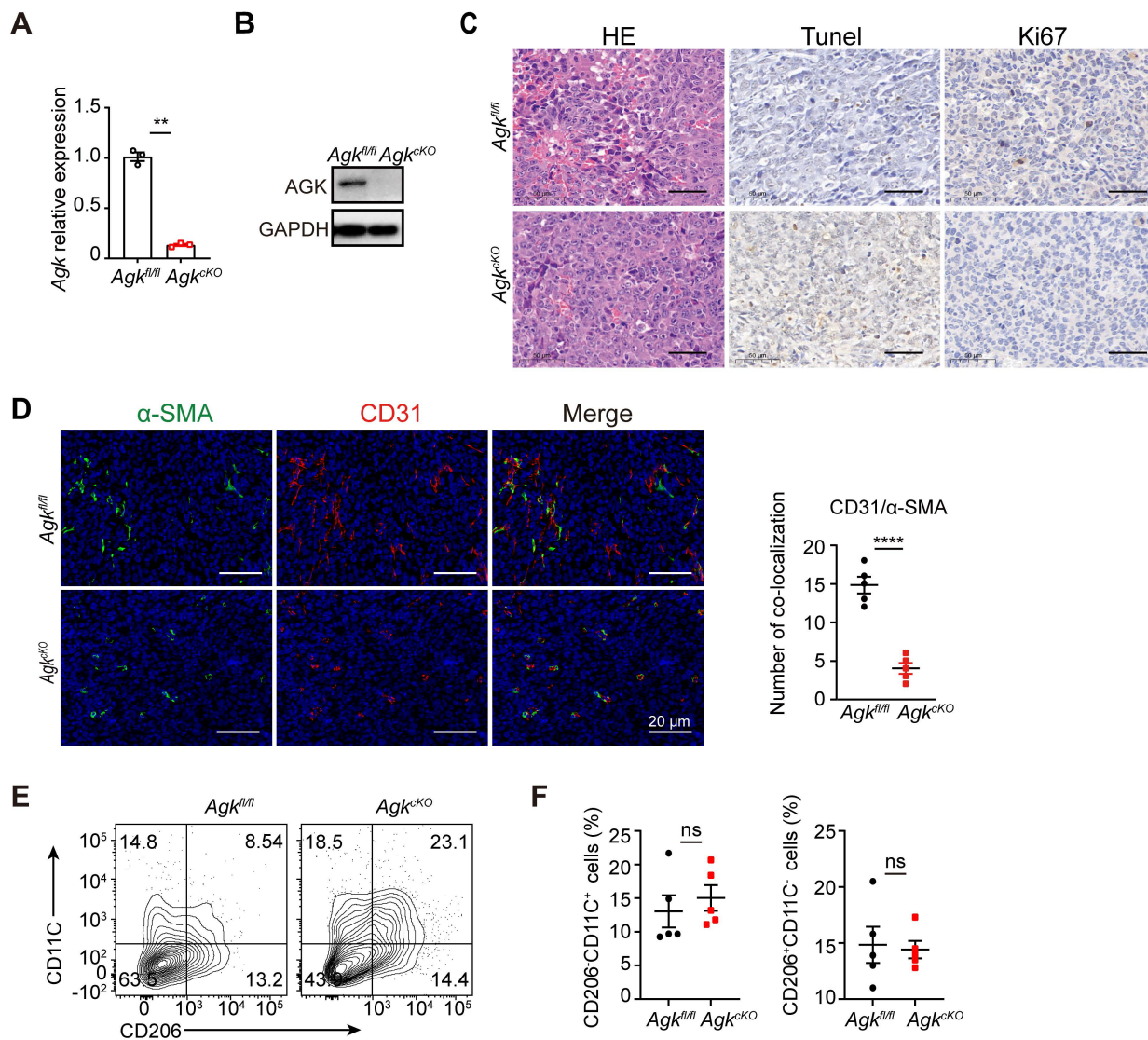


Figure S2

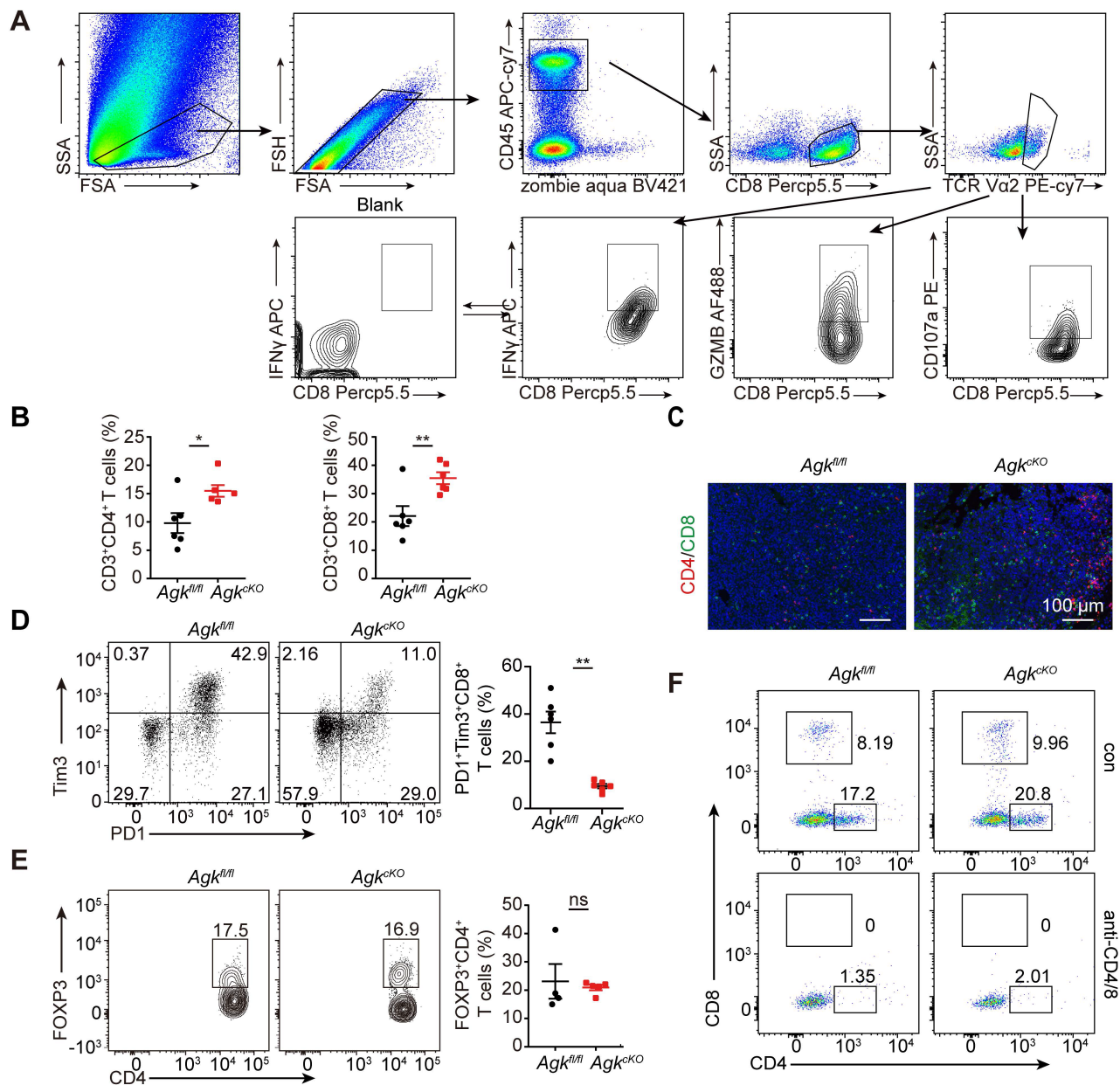


Figure S3

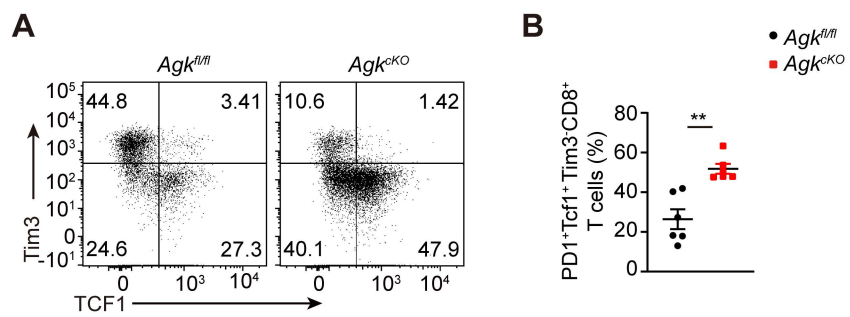


Figure S4

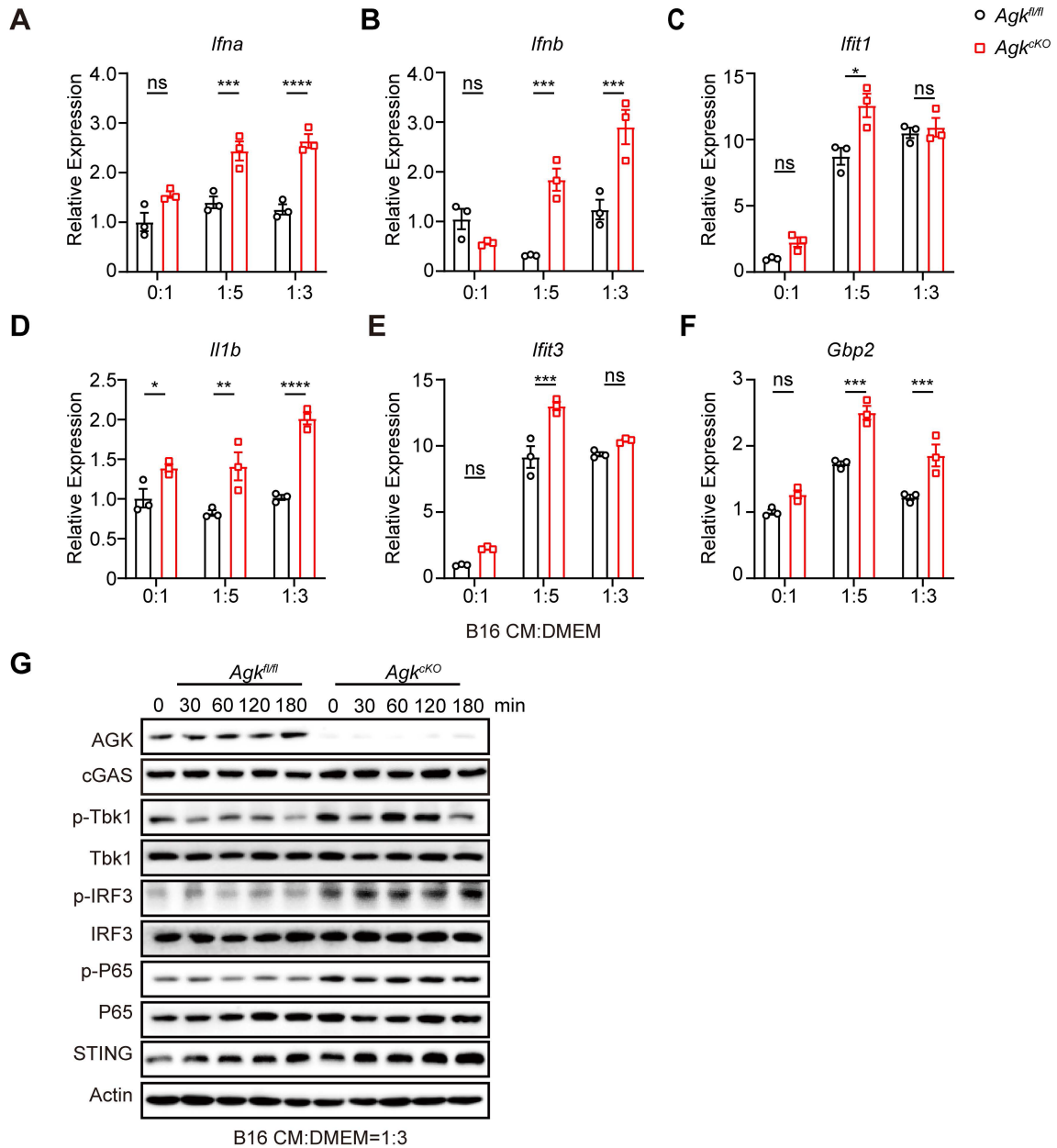
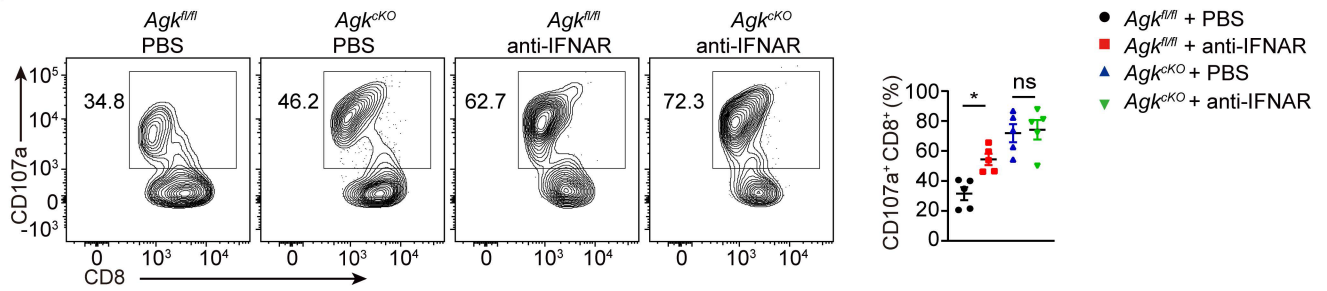


Figure S5

A



B

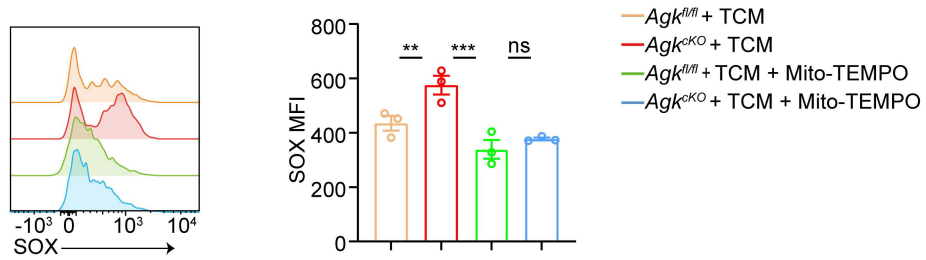


Table S1. Oligonucleotide primers for qPCR

Target	Sequence
Mouse-Agk (F)	TTTGAGTCATACCCTCTTTGCC
Mouse-Agk (R)	TCAAGTGGAAGTGTCTCTCCTT
Mouse-Ifna (F)	GCTTTCCTGATGGTTTTGGTG
Mouse-Ifna (R)	AGGCTTTCTTGTCCTGAGG
Mouse-Ifnb (F)	CCAGCTCCAAGAAAGGACGA
Mouse-Ifnb (R)	TGGATGGCAAAGGCAGTGTA
Mouse-Ifit1 (F)	AGAGTCAAGGCAGGTTTCTG
Mouse-Ifit1 (R)	TGTGAAGTGACATCTCAGCTG
Mouse-Il1b (F)	GCAACTGTTCCCTGAACTCAACT
Mouse-Il1b (R)	ATCTTTTGGGGTCCGTCAACT
Mouse-Ifit3 (F)	CTGAAGGGGAGCGATTGATT
Mouse-Ifit3 (R)	AACGGCACATGACCAAAGAGTAGA
Mouse-Gbp2 (F)	CTGCACTATGTGACGGAGCTA
Mouse-Gbp2 (R)	GAGTCCACACAAAGGTTGGAAA
Mouse-mtDNA Dloop1 (F)	AATCTACCATCCTCCGTGAAACC
Mouse-mtDNA Dloop1 (R)	TCAGTTTAGCTACCCCAAGTTTAA
Mouse-mtDNA Dloop2 (F)	CCCTTCCCCATTTGGTCT
Mouse-mtDNA Dloop2 (R)	TGGTTTCACGGAGGATGG
Mouse-mtDNA 16S (F)	CACTGCCTGCCCAGTGA
Mouse-mtDNA 16S (R)	ATACCGCGCCGTTAAA
Mouse-mtDNA ND4 (F)	AACGGATCCACAGCCGTA
Mouse-mtDNA ND4 (R)	AGTCCTCGGGCCATGATT